Article:
Azizi, S orcid.org/0000-0002-9274-1177 and Sanaye-Pasand, M (2017) From Available Synchrophasor Data to Short-Circuit Fault Identity: Formulation and Feasibility Analysis. IEEE Transactions on Power Systems, 32 (3). pp. 2062-2071. ISSN 0885-8950

https://doi.org/10.1109/TPWRS.2016.2608927

From Available Synchrophasor Data to Short-Circuit Fault Identity: Formulation and Feasibility Analysis

Sadegh Azizi, Student Member, IEEE, Majid Sanaye-Pasand, Senior Member, IEEE

Abstract—This paper proposes a novel formulation for determining the short-circuit fault identity, that is the fault type, faulted line and exact fault distance on it, by using available synchrophasor data. A simple and yet quite effective procedure is developed to model the fault area as a stand-alone sub-system. Thanks to phasor measurement units (PMUs), the proposed technique does not require the operating point and model of the portions being replaced. This greatly alleviates the complexity and technical problems involved in modeling the entire power system, as enforced by existing wide-area methods. A couple of effective theorems in Circuit Theory are exploited in a way as to make the pre-fault bus impedance matrix applicable in the post-fault condition. The obtained fault equations are readily solved by the least-squares method to provide a closed-form solution for the fault distance. Two necessary and sufficient conditions are introduced to assess the fault location feasibility by a given set of PMUs. High accuracy is achieved since the calculations merely involve sound equations remaining after removing erroneous measurements of instrument transformers. The proposed method is successfully validated by more than 10000 simulation cases conducted on the New England 39-bus and 118-bus test systems.

Index Terms—Phasor measurement unit (PMU), least-squares method, system of linear equations, wide-area fault location.

I. Introduction

SUBSEQUENT to a short-circuit fault, current and voltage waveforms vary over a wide range at different locations of the power system [1]. Phasor measurement units (PMUs), as the building blocks of wide-area systems, make it possible to measure, time-stamp and transmit the fundamental-frequency phasors of these signals to the control center. Wide-area fault location is the process of determining the fault identity, i.e., the fault type, faulted line and exact fault distance on it, by using the data of a limited number of PMUs.

Signals fed to PMUs through instrument transformers are not ideal, and hence, their extracted synchrophasors would contain some errors. Under transient conditions, the signal transformation would get even worse [1]. The larger the change a current transformer (CT) or a capacitive voltage transformer (CVT) undergoes, the less successful it would be in reproducing an exact replica of its primary input [2]. This implies an inherent advantage of wide-area applications over local practices since the measurement devices located farther from the fault point experience smaller changes upon a fault.

Conventional fault location methods often use a minimal number of equations constructed based on the measured quantities at the faulted line terminals [3]-[14]. If any of the measurement devices is unable to faithfully provide the related quantity, the fault equations involving that quantity become erroneous. This would make fault location inaccurate or even infeasible due to lack of enough independent equations. Travelling wave-based wide-area fault location methods require measurement devices of very high sampling rate to be deployed [15], [16]. Phasor-based wide-area fault location is a viable solution to this problem, since it uses the entire redundant fault equations constructed over the available PMU data [17]-[31]. However, the existing phasor-based wide-area methods require the parameters and topology data of the whole system for pinpointing the fault. On the other hand, nonlinear formulation and/or iterative nature of these methods make it very difficult to deal with imperfect measurements, in addition to enforcing a demanding solving process [20].

It is neither necessary nor even useful to model the entire power system with full details in order to study a short-circuit fault. Rather, it is more practical to only focus on the region where the fault is located. In doing so, the conventional network reduction technique can be used. This would add some transfer links to the system whose number is proportional to the square of the number of boundary terminals. Not only is this somehow in opposition with the primary objective of network reduction, but also it requires some information from the portions being replaced [32].

An innovative technique is proposed in this paper to represent the remaining system seen from the fault area boundaries without requiring its parameters and operating point. The resulting sub-system would be much easier to analyze and still involves reliable measurements. Moreover, the proposed framework enables the use of pre-fault bus impedance matrix even after fault occurrence. Accordingly, the fault equations become linear, and hence, can be readily solved to determine the fault identity. Besides, bad data detection techniques can be incorporated in such a linear framework for removing erroneous measurements of instrument transformers. Two necessary and sufficient conditions are also introduced in this paper to assess the fault location feasibility. The associated procedure is shown to be independent of the exact fault distance on the faulted line and thus can be carried out offline for any given set of PMUs.

The rest sections of this paper are organized as follows. Section II describes fault areas of interest to this study and elaborates on how to model them as a stand-alone fault sub-system. Section III proposes a linear framework comprising all extractable fault equations over PMU data. Extensive simulation studies are conducted and discussed in Section IV. Finally, the paper is concluded in Section V.

This work was supported by the University of Tehran under Grant 8101064-1-09.

The authors are with the School of Electrical and Computer Engineering, College of Engineering, University of Tehran, Tehran 14395-515 Iran (e-mail: sadegh.azizi@ut.ac.ir; msanaye@ut.ac.ir).

II. Extraction of Fault Sub-System

In this section, a technique is proposed to model the fault area as a stand-alone sub-system. As a great advantage, this technique does not require the operating point and parameters of the portions being replaced. The sufficient and necessary conditions of being able to locate the fault in the fault sub-system are introduced later. It is possible to devise an optimal PMU placement algorithm to meet those conditions [33]. However, due to space limit, this paper is confined to fault location using the PMUs already installed in the system.

A. Fault Area Definition

To reduce the computational complexity of fault analysis, and also to simplify the exchange and processing of data between utilities, a large power system can judiciously be divided into several areas [32], [33]. In doing so, geographical closeness, system topology and other technical criteria can be coupled with engineering judgment. The area including a short-circuit fault is called the fault area.

From the fault area perspective, various components of the system can be divided into either internal or external components. The links (transmission lines and transformers) connecting internal terminals to external ones are called interconnection links. Based on the substitution theorem, every interconnection link can be replaced with a suitably adjusted current source [34]. As will be shown in this paper, such a possibility is quite beneficial when the amounts of these sources are known.

B. Modeling the Fault Area as a Stand-Alone Sub-System

To derive the linear framework for fault location, it is assumed for the moment that the fault has happened in an area the currents of whose connections with the remaining system are measured by PMUs. Cases in which the boundary terminals are not entirely monitored by PMUs are also studied later.

In fault analysis, electric machines are each modeled as a constant voltage source in series with a fixed impedance. Such an approximation serves well for fault calculations. According to the Thevenin-Norton equivalent theorem, this model can be converted to an equivalent constant current source in parallel with that impedance [34]. Providing more accuracy, an electric machine can be entirely replaced with an equivalent current or voltage source with no approximation. This can be accomplished by measuring that machine current injection or its terminal voltage using a PMU.

Assume B is the set of all terminals and B_{FA} is the set of internal ones, i.e., those located in the fault area. Let $J_{s,r}$ denote the sending-end current phasor of link s-r. For the sake of generality, this variable is assigned a zero value if terminals s and r are not connected to each other. Interconnection links and electric machine(s) at the boundary terminal k can be substituted altogether with a single current source injecting an identical amount of current. In general, bus injected currents for the PMU-equipped boundary terminals are obtained from

$$I_k = I_k^m - \sum_{r \in \{B - B_{FA}\}} J_{k,r}\,, \qquad \forall 1 \le k \le Nb \tag{1}$$

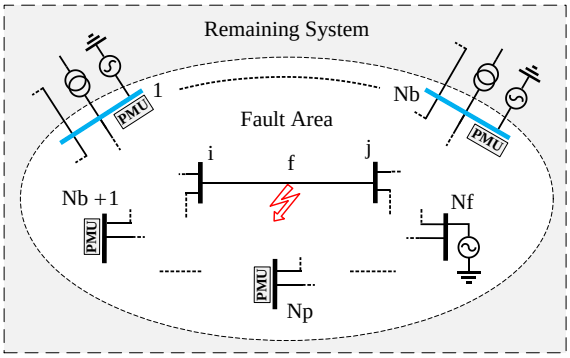

Fig. 1. A short-circuit fault on line i-j in the fault area.

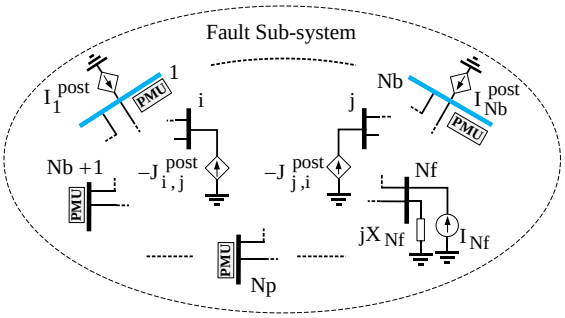

Fig. 2. Fault sub-system derived by replacing the remaining system and the faulted line with suitable current sources.

where I_k^m is the sum of currents of machines at terminal k, and 1 to Nb are the indices of boundary terminals.

All the boundary terminals of the fault area, shown in Fig. 1 in blue color, are equipped with PMUs. It is possible to convert this fault area into a stand-alone sub-system, as explained. Fig. 2 shows the resulting fault sub-system with Nf terminals among which Np terminals are PMU-equipped. If an electric machine is connected to a terminal with no PMU, e.g., terminal Nf, that machine would be modeled as a constant current source in parallel with a suitable impedance.

III. Fault Location in the Fault Sub-System

In power system analysis, the bus impedance matrix is commonly used to obtain the current and voltage signals at different locations. For a fault, the fault distance and resistance have to be considered in constructing the bus impedance matrix, regardless of whether they are among the unknowns to be calculated. Fault equations are highly nonlinear in terms of these unknowns and thereby demand considerable computational effort to be solved. In this section the faulted line is substituted with two suitable current sources in terms of that the fault equations become linear.

A. Derivation of Fault Equations

The difference between pre- and post-fault signals, commonly referred to as superimposed components, is used here to derive the fault equations and develop a linear framework for wide-area fault location. To start with, the nodal equations for the fault sub-system prior to the fault is written in the matrix form as

$$\mathbf{V}^{pre} = \mathbf{Z}^{pre}\mathbf{I}^{pre}\,, \tag{2}$$

where $\mathbf{Z}^{pre}$ is the bus impedance matrix in the pre-fault condition and $\mathbf{V}^{pre}$ is the Nf×1 vector of pre-fault bus voltage phasors. In addition, $\mathbf{I}^{pre}=[I_1^{pre},\ldots,I_{Nf}^{pre}]^T$ is the vector of bus injected currents where the pre-fault nodal current at bus k is denoted by I_k^{pre}.

On the other hand, line i-j can be replaced with two current sources injecting currents $-J_{i,j}^{pre}$ and $-J_{j,i}^{pre}$ to the respective terminals, in the pre-fault condition. Accordingly,

$$\mathbf{V}^{pre}=\mathbf{Z}^{(i,j)}\mathbf{I}^{pre(i,j)} \tag{3}$$

where the superscript (i,j) is used to denote the related parameter or variable while line i-j has been replaced with two equivalent current sources. Accordingly,

$$\mathbf{I}^{pre(i,j)}=\left[I_1^{pre}\ \ldots,I_i^{pre}-J_{i,j}^{pre},\ldots,I_j^{pre}-J_{j,i}^{pre},\ldots I_{Nf}^{pre}\right]^T. \tag{4}$$

An equation similar to (3) can be derived for the post-fault condition as follows

$$\mathbf{V}^{post}=\mathbf{Z}^{(i,j)}\mathbf{I}^{post(i,j)} \tag{5}$$

where

$$\mathbf{I}^{post(i,j)}=\left[I_1^{post},\ldots,I_i^{post}-J_{i,j}^{post},\ldots,I_j^{post}-J_{j,i}^{post},\ldots I_{Nf}^{post}\right]^T. \tag{6}$$

It should be noted that the bus impedance matrix $\mathbf{Z}^{(i,j)}$ remains unchanged even after the fault occurrence. This technique was firstly proposed in [20], and is used here for fault location in the fault area using both voltage and current synchrophasors. To this end, the nodal equations for the superimposed fault sub-system is obtained by subtracting (3) from (5) as

$$\Delta\mathbf{V}=\mathbf{Z}^{(i,j)}\Delta\mathbf{I}-\begin{bmatrix}Z_{1,i}^{(i,j)} & Z_{1,j}^{(i,j)}\\ \vdots & \vdots\\ Z_{Nf,i}^{(i,j)} & Z_{Nf,j}^{(i,j)}\end{bmatrix}\begin{bmatrix}\Delta J_{i,j}\\ \Delta J_{j,i}\end{bmatrix}. \tag{7}$$

As can be seen from (7), the superimposed voltages are functions of both the superimposed nodal currents, and superimposed current sources substituted for the faulted line.

Assume the superimposed voltages at terminals 1 to Np are directly measured by PMUs. Each of these measured values can be set equal to its corresponding parametric expression on the left-hand side of (7). To distinguish between the measured and true values, the superscript "*meas*" is used for the measured ones hereinafter. For non-boundary terminals, the nodal injection is either zero or remains identical before and after the fault inception. Thus, the kth equation in (7) can be expanded as

$$\Delta V_k^{meas}=\sum_{q=1}^{Nb}Z_{k,q}^{(i,j)}\Delta I_q-Z_{k,i}^{(i,j)}\Delta J_{i,j}-Z_{k,j}^{(i,j)}\Delta J_{j,i}+e_{V(k)},\quad\forall 1\le k\le Np. \tag{8}$$

where $e_{V(k)}$ represents the error between the measured voltage at terminal k and its true value.

Being directly measured, none of the fault-area parameters is used to obtain the value of current sources representing the external system. Considering the possible measurement errors, these values are also incorporated within the unknowns to be calculated. In this respect, an equation can be constructed over the measured and true values of the current source at the boundary terminal k as

$$\Delta I_k^{meas}=\Delta I_k+e_{I(k)},\qquad\forall 1\le k\le Nb \tag{9}$$

where $e_{I(k)}$ represents the error between the sum of measured currents entering the boundary terminal k and its true value.

For an internal superimposed current measurement (within the fault area), the measured value can be expressed as a function of the superimposed current sources at the boundary and faulted line terminals. Let J_k denote the sending-end current of the healthy line k connecting terminals u and w. Besides, let $l_{u,w}$, $Z_{u,w}^c$ and $\gamma_{u,w}$ denote that line's length, characteristic impedance and propagation constant, respectively. Using the distributed-parameter line model, the superimposed current of the sending-end of line k is expressed here in terms of its terminal superimposed voltages as

$$\Delta J_k^{meas}=\frac{\Delta V_u}{Z_{u,w}^c}\tanh\left(\frac{\gamma_{u,w}l_{u,w}}{2}\right)+\frac{\Delta V_u-\Delta V_w}{Z_{u,w}^c\sinh\left(\gamma_{u,w}l_{u,w}\right)}. \tag{10}$$

Substituting the superimposed voltages from (7) into (10),

$$\Delta J_k^{meas}=\sum_{q=1}^{Nb}C_{k,q}^{(i,j)}\Delta I_q-C_{k,i}^{(i,j)}\Delta J_{i,j}-C_{k,j}^{(i,j)}\Delta J_{j,i}+e_{J(k)} \tag{11}$$

where

$$C_{k,q}^{(i,j)}=\frac{Z_{u,q}^{(i,j)}}{Z_{u,w}^c\tanh\left(\gamma_{u,w}l_{u,w}\right)}-\frac{Z_{w,q}^{(i,j)}}{Z_{u,w}^c\sinh\left(\gamma_{u,w}l_{u,w}\right)}. \tag{12}$$

The linear equation (11) obtained above is valid only for healthy lines. Existence of a fault at an unknown distance on the faulted line makes it impossible to express the current of that line only in terms of its terminal voltages. Nevertheless, if any of the faulted line terminals, say terminal i, is PMU-equipped, the current flowing from that side is directly measured. Thus, an equation similar to (9) can be derived as

$$\Delta J_{i,j}^m=\Delta J_{i,j}+e_{i,j} \tag{13}$$

where $e_{i,j}$ denotes the error between the measured and true values. A similar equation could be also written for the current flowing from the terminal j side of the faulted line, if that side of the line is also equipped with a PMU.

Assume Nl is the number of transmission line terminals in the fault area whose current phasors are measured by PMUs. Additionally, Nh is assumed to be the number of healthy line terminals whose current phasors are measured by PMUs. Considering all constructible equations in any form of (8), (9), (11) and (13), a system of Ns linear equations in (Nb+2) unknowns can be developed where Ns=Np+Nb+Nl. This system of equations would have a matrix form of

$$\underset{Ns\times 1}{\mathbf{M}}=\underset{Ns\times(Nb+2)}{\mathbf{H}}\ \underset{(Nb+2)\times 1}{\mathbf{X}}=\underset{Ns\times 2}{\mathbf{H}^J}\begin{bmatrix}\Delta J_{i,j}\\ \Delta J_{j,i}\end{bmatrix}+\underset{Ns\times Nb}{\mathbf{H}^I}\left[\Delta I_1\ \ \ldots\ \ \Delta I_{Nb}\right]^T, \tag{14}$$

where **M** and **H** are the measurement and coefficient matrices, respectively. Besides, **X** is the vector of unknowns composed of superimposed current sources substituted at the boundary terminals and the faulted line terminals.

The obtained system of linear equations above contains all extractible fault equations in the fault area, with respect to available synchrophasor measurements. This system has been constructed based on the earlier assumption that all boundary terminals are equipped with PMUs. If this is not the case for

any of the boundary terminals, the associated equations must be removed from the equation set. Either of the last two rows of (14) must be excluded if the corresponding terminal of the faulted line is not equipped with a PMU to measure the respective current. This system is rewritten explicitly in (15).

B. Determining the Fault Identity

The fault identity, i.e., the faulted line, fault type and distance is determined here. The unknown vector **X**, being the superimposed currents, can be readily calculated by solving (14) using the least-squares method as [35]

$$\hat{\mathbf{X}} = \left(\mathbf{H}^{\mathrm{T}}\mathbf{H}\right)^{-1}\mathbf{H}^{\mathrm{T}}\mathbf{M} \ . \tag{16}$$

The hat symbol on **X** demonstrates that this estimate of unknowns would have a difference with its true value as a result of measurement errors. The vector of residuals for this system is defined as $\mathbf{r} = \mathbf{M}\text{-}\mathbf{H}\hat{\mathbf{X}}$.

The estimated fault distance in each sequence network would be equal to the actual value if the impedance matrix of that network is accurate. However, it is difficult to obtain an accurate and reliable zero-sequence network in practice [2], [32]. Accordingly application of the zero-sequence network is better to be avoided, to preserve the fault location accuracy [20]. Thus, (14) is constructed and solved only for the positive- and negative-sequence networks in this paper. Then, the average of obtained distances considered as the fault location. The sum of squared residuals corresponding to the faulted line is noticeably smaller than that of the other lines. The reason is because the faulted line is the only one for that (14) has been constructed and holds. Accordingly, the faulted line can be easily identified by calculating this value for all the suspected lines in the fault area.

In the next step, the voltage at the faulted line terminals can be derived from (7) as

$$\Delta\hat{V}_i = \sum_{q=1}^{Nb} Z_{i,q}^{(i,j)}\Delta\hat{I}_q - Z_{i,i}^{(i,j)}\Delta\hat{J}_{i,j} - Z_{i,j}^{(i,j)}\Delta\hat{J}_{j,i} \ , \tag{17}$$

$$\Delta\hat{V}_j = \sum_{q=1}^{Nb} Z_{j,q}^{(i,j)}\Delta\hat{I}_q - Z_{j,i}^{(i,j)}\Delta\hat{J}_{i,j} - Z_{j,j}^{(i,j)}\Delta\hat{J}_{j,i} \ . \tag{18}$$

To this point, the superimposed voltages and currents at the faulted line terminals have been calculated for positive- and negative-sequence networks. The superimposed two-terminal fault location formula (19) can be applied to each of the superimposed sequence networks to obtain the fault distance [20]. If the negative- and zero-sequence quantities measured by PMUs are very small, it is concluded that the fault is symmetrical (3-ph). Otherwise, the superimposed positive- and negative-sequence currents at the fault point should be calculated from both sides of the faulted line [20]. From the sequence networks interconnection for asymmetrical faults, it follows that for 1-ph-g and 2-ph-g faults $I_f^p = I_f^n$ and $I_f^p \neq I_f^n$, respectively. In the special case of 2-ph faults $I_f^p = -I_f^n$. Accordingly, the fault type can be readily identified despite circumventing zero-sequence quantities.

C. Fault Location Feasibility Analysis

The fault location feasibility analysis refers to assessment of whether the superimposed signals at the faulted line terminals, and hence the fault distance can be uniquely obtained from (14), (17) and (18) using the available PMUs. The system of equations (14) has at least one solution being the superimposed signals sensed subsequent to the fault. The vector of unknowns **X** can be uniquely obtained from this system if the coefficient matrix **H** has full rank. Afterwards, the superimposed voltages $\Delta\hat{V}_i$ and $\Delta\hat{V}_j$ can be obtained from (17) and (18) by inserting the calculated $\Delta\hat{J}_{i,j}, \Delta\hat{J}_{j,i}, \Delta\hat{I}_1, \ldots, \Delta\hat{I}_{Nb}$ in those equations.

The main question arising here is what happens to the problem when **H** is rank deficient. In other words, it is desirable to know whether or not **H** being of full rank is a necessary condition for fault location to be feasible. This would be the case when (14) essentially does not involve enough independent equations or some of its equations are excluded for being bad data. To answer this question, it should be recalled that in the reduced row echelon form of a matrix, the first nonzero entry in each nonzero row is called pivot and

$$\begin{bmatrix} \Delta V_1^{meas} \\ \vdots \\ \Delta V_{Np}^{meas} \\ \Delta I_1^{meas} \\ \vdots \\ \Delta I_{Nb}^{meas} \\ \Delta J_1^{meas} \\ \vdots \\ \Delta J_{Nh}^{meas} \\ \Delta J_{i,j}^{meas} \\ \Delta J_{j,i}^{meas} \end{bmatrix} = \begin{bmatrix} -\begin{bmatrix} Z_{1,i}^{(i,j)} & Z_{1,j}^{(i,j)} \\ \vdots & \vdots \\ Z_{Np,i}^{(i,j)} & Z_{Np,j}^{(i,j)} \end{bmatrix} & \begin{bmatrix} Z_{1,1}^{(i,j)} & \vdots & Z_{1,Nb}^{(i,j)} \\ \vdots & \ddots & \vdots \\ Z_{Np,1}^{(i,j)} & \cdots & Z_{Np,Nb}^{(i,j)} \end{bmatrix} \\ [\mathbf{0}]_{(Nb\times 2)} & [\mathbf{I}]_{(Nb\times Nb)} \\ -\begin{bmatrix} C_{1,i}^{(i,j)} & C_{1,j}^{(i,j)} \\ \vdots & \vdots \\ C_{Nh,i}^{(i,j)} & C_{Nh,j}^{(i,j)} \end{bmatrix} & \begin{bmatrix} C_{1,1}^{(i,j)} & \vdots & C_{1,Nb}^{(i,j)} \\ \vdots & \ddots & \vdots \\ C_{Nh,1}^{(i,j)} & \cdots & C_{Nh,Nb}^{(i,j)} \end{bmatrix} \\ [\mathbf{I}]_{(2\times 2)} & [\mathbf{0}]_{(2\times Nb)} \end{bmatrix} \times \begin{bmatrix} \Delta J_{i,j} \\ \Delta J_{j,i} \\ \Delta I_1 \\ \vdots \\ \Delta I_{Nb} \end{bmatrix} + \begin{bmatrix} e_{V(1)} \\ \vdots \\ e_{V(Np)} \\ e_{I(1)} \\ \vdots \\ e_{I(Nb)} \\ e_{J(N1)} \\ \vdots \\ e_{J(Nh)} \\ e_{i,j} \\ e_{j,i} \end{bmatrix} \tag{15}$$

$$\alpha_{i,j} = \frac{1}{\gamma_{i,j} l_{i,j}} \times \tanh^{-1}\left(\frac{\cosh(\gamma_{i,j} l_{i,j})\Delta\hat{V}_j - Z_{i,j}^{c} \sinh(\gamma_{i,j} l_{i,j})\Delta\hat{J}_{j,i} - \Delta\hat{V}_i}{\sinh(\gamma_{i,j} l_{i,j})\Delta\hat{V}_j - Z_{i,j}^{c} \cosh(\gamma_{i,j} l_{i,j})\Delta\hat{J}_{j,i} - Z_{i,j}^{c}\Delta\hat{J}_{i,j}} \right) \tag{19}$$

has a value of 1. The corresponding variable to each pivot in the reduced echelon form of the coefficient matrix has a unique solution if and only if all the other entries to its right are zero [36]. In fact, this might be the case for some pivots and not all of them. In such a case, it is only possible to extract a unique solution for the corresponding unknowns while the whole system has infinitely many solutions [36].

Now, let assume $\Delta J_{i,j}$ and $\Delta J_{j,i}$ are uniquely obtainable from (14). Accordingly, a new system of equations can be extracted from (14) as below

$$\mathbf{H}^{I}\left[\Delta I_1 \quad ,\ldots, \quad \Delta I_{Nb}\right]^{T} = \underbrace{\mathbf{M}-\mathbf{H}^{J}\left[\Delta J_{i,j} \quad \Delta J_{j,i}\right]^{T}}_{\boldsymbol{\Psi}}, \qquad (20)$$

where the terms on the right-hand side construct a known vector that is named $\boldsymbol{\Psi}$. Without further analysis, it is not possible to say whether or not (20) is uniquely solvable for its unknowns, i.e., the superimposed current sources at the boundary terminals.

The value of every single current source at the boundary terminals is of no direct concern, as far as the superimposed voltages at the faulted line terminals are to be calculated. To demonstrate this point, the coefficient matrix $\mathbf{H}^{I}$ is first decomposed into $1\times Nb$ row vectors of $\mathbf{h}_1^{I},\ldots,\mathbf{h}_{Ns}^{I}$. Now a state is considered in which the row vector $\boldsymbol{\Upsilon}_{i,j}^{Nb}=\left[Z_{i,1}^{(i,j)},\ldots,Z_{i,Nb}^{(i,j)}\right]$ can be written as a linear combination $a_1\mathbf{h}_1^{I}+\ldots+a_{Ns}\mathbf{h}_{Ns}^{I}$, where $a_1,\ldots,a_{Ns}$ are complex scalars. With respect to (17) and (20), the superimposed voltage at terminal i would be calculated from

$$\Delta\hat{V}_i=\left[a_1\ ,\ldots,\ a_{Ns}\right]\boldsymbol{\Psi}-\left[Z_{i,i}^{(i,j)}\ \ Z_{i,j}^{(i,j)}\right]\begin{bmatrix}\Delta\hat{J}_{i,j}\\ \Delta\hat{J}_{j,i}\end{bmatrix}. \qquad (21)$$

The superimposed voltage at terminal j can be obtained by a similar procedure as

$$\Delta\hat{V}_j=\left[b_1\ ,\ldots,\ b_{Ns}\right]\boldsymbol{\Psi}-\left[Z_{j,i}^{(i,j)}\ \ Z_{j,j}^{(i,j)}\right]\begin{bmatrix}\Delta\hat{J}_{i,j}\\ \Delta\hat{J}_{j,i}\end{bmatrix}, \qquad (22)$$

where it has been assumed that $\boldsymbol{\Upsilon}_{j,i}^{Nb}=\left[Z_{j,1}^{(i,j)},\ldots,Z_{j,Nb}^{(i,j)}\right]$ can be written as the linear combination $b_1\mathbf{h}_1^{I}+\ldots+b_{Ns}\mathbf{h}_{Ns}^{I}$.

It follows from (21) and (22) that the superimposed voltages at the faulted line terminals can be obtained if $\boldsymbol{\Upsilon}_{i,j}^{Nb}$ and $\boldsymbol{\Upsilon}_{j,i}^{Nb}$ are linear combinations of vectors $\mathbf{h}_1^{I},\ldots,\mathbf{h}_{Ns}^{I}$. This does not imply in any way that every single current source at the boundary terminals has to be uniquely obtainable. Thus, for fault location by the proposed method, it is not necessary that (14) be uniquely solvable, or equivalently, **H** be of full rank.

Accordingly, the fault location on line i-j can be determined if the two necessary and sufficient conditions below hold:
Condition I: The reduced row echelon form of **H** includes two pivots corresponding to $\Delta J_{i,j}$ and $\Delta J_{j,i}$. These pivots are the only nonzero entries in their containing rows and columns.
Condition II: Either of the two row vectors $\boldsymbol{\Upsilon}_{i,j}^{Nb}$ and $\boldsymbol{\Upsilon}_{j,i}^{Nb}$, can be written as a linear combination of $\mathbf{h}_1^{I},\ldots,\mathbf{h}_{Ns}^{I}$. Hence,

$$\operatorname{rank}\left(\left[\mathbf{H}^{I};\ \boldsymbol{\Upsilon}_{i,j}^{Nb};\ \boldsymbol{\Upsilon}_{j,i}^{Nb}\right]\right)=\operatorname{rank}\left(\mathbf{H}^{I}\right). \qquad (23)$$

It follows from Condition I that the superimposed currents at the faulted line terminals would be uniquely obtained from (14). Condition II together with Condition I guarantees that the superimposed voltages at those locations can be also calculated from (21) and (22). Accordingly, if the both conditions hold, the fault distance on line i-j can be readily obtained from the closed-form solution (19). This is the case regardless of the rank of **H**. On the other hand, it can be shown that if **H** is of full rank, Conditions I and II both hold. Based on the described findings, **H** being of full rank is only a sufficient and not a necessary condition for fault location to be feasible. Therefore, if only this condition is checked to evaluate the fault location feasibility, a number of acceptable states may be overlooked.

The pre-fault bus impedance matrix suffices for evaluating the introduced conditions. Thus, the feasibility of fault location on each line is independent of the fault type, resistance and exact fault distance on that line. By reduction in the number of independent equations, fault location would become infeasible for some lines while remaining viable for the rest. This might happen due to inclusion of bad data in the measurement set, or not having some of the boundary terminals monitored by PMUs. It can be also concluded that the fault distance on a line might be obtainable although the entire boundary terminals are not equipped with PMUs.

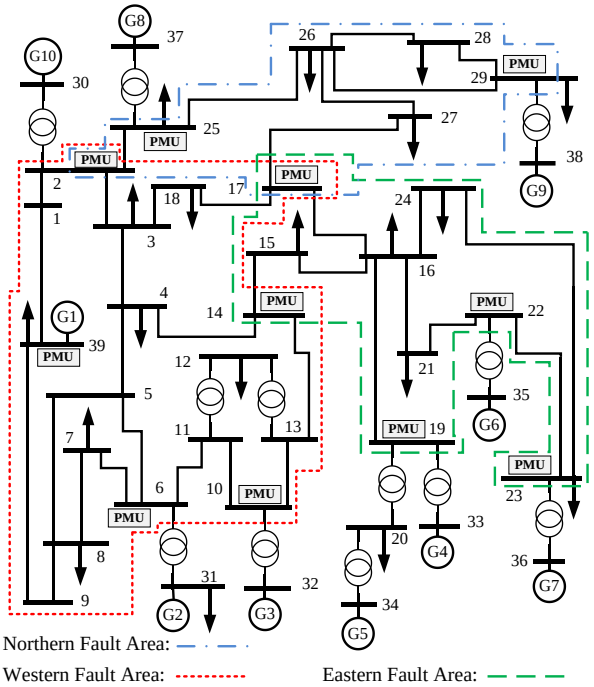

Fig. 3. Single line diagram of 39-bus system.

IV. Simulation Results

To evaluate the performance of the proposed wide-area fault location method, numerous simulation studies are conducted on the New England 39-bus and 118-bus systems [37]. The situation in which boundary terminals are partly monitored by PMUs is also studied in this section. The single line diagram of the 39-bus system is shown in Fig. 3.

The DIgSILENT power factory software [38] is used to model the 39-bus system and simulate short-circuit faults on

TABLE I
FAULT LOCATION RESULTS FOR VARIOUS FAULTS ON LINE 21-22

Fault Distance (%)	5	10	20	30	40	50	60	70	80	90	95
	Average Estimation Error (%)										
Proposed	0.07	0.06	0.04	0.04	0.04	0.02	0.03	0.03	0.04	0.05	0.05
Ref. [3]	1.12	0.64	0.39	0.36	0.04	0.03	0.03	0.13	0.19	2.21	3.98
Ref. [4]	0.96	0.51	0.36	0.29	0.08	0.06	0.07	0.12	0.22	1.62	3.17
Ref. [5]	1.43	0.75	0.41	0.24	0.04	0.05	0.05	0.18	0.21	1.60	3.54
Ref. [6]	2.29	1.25	0.76	0.61	0.12	0.09	0.10	0.11	0.18	1.95	4.43

it. The outputs of instrument transformers are passed through a third-order Butterworth anti-aliasing filter. The signals are sampled with a sampling rate of 2500 Hz, i.e., 50 samples per cycle and their fundamental-frequency phasors are extracted using discreet Furrier transform. By calculating symmetrical components of the obtained synchrophasors, system of equation (15) is constructed and individually solved for any of the three sequence networks. The three estimated fault distances would be ideally equal. However, in practice, the zero-sequence network is not adequately accurate because of technical problems such as difficulties in measuring ground impedance [20]. Hence, in this paper, the fault distance is calculated merely in positive- and negative-sequence networks and the obtained results are averaged to increase the estimation reliability.

The fault location is estimated by the proposed method, while bad data in the measurement set is identified and eliminated by using the largest normalized residual test [35].The estimation error is finally calculated as

$$\text{Estimation Error}(\%) = \left|\frac{\text{Estimated FL-Actual FL}}{\text{Faulted Line Length}}\right| \times 100. \quad (24)$$

A. Wide-Area vs. Conventional Fault Location

The use of magnetic-core instrument transformers makes the calculated phasors not exactly match their true values in the steady-state condition. In transient conditions, the amount of dissimilarity increases considerably. This would adversely affect the accuracy of fault location using the conventional methods. However, erroneous measurements can be identified and removed by wide-area fault location in virtue of inclusion of sufficiently independent fault equations, thereby ensuring the estimation accuracy.

Table I provides the average estimation errors obtained by the proposed and a number of other fault location methods for more than 1000 fault cases. These cases are simulated at several distances on line 21-22, by varying the fault type, resistance and inception angle. For faults close to either of the line terminals, the CVT at that terminal exhibits a more severe subsidence transient. Due to the large magnitude of the flowing current, it is more likely for the CT to go into significant saturation for faults close to terminal 22. These are the reasons for which the conventional methods [3-6] provide inaccurate results in the case of faults close to the line terminals.

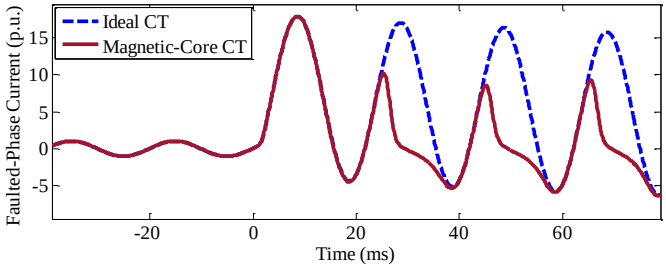

Fig. 4. Faulted-phase current obtained using ideal and magnetic-core current transformers at terminal 22.

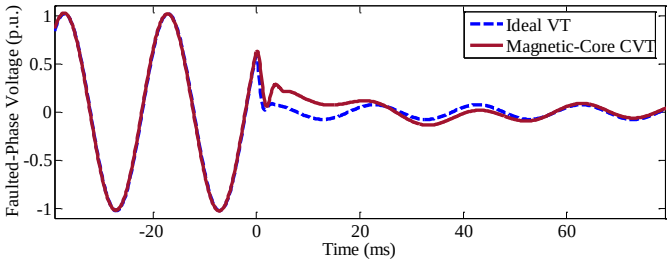

Fig. 5. Faulted-phase voltage obtained using ideal and magnetic-core capacitive voltage transformers at terminal 22.

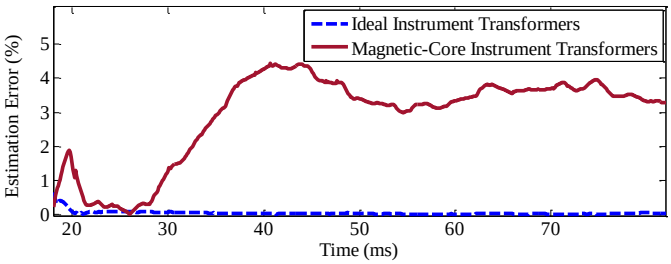

Fig. 6. Estimation error of the conventional two-terminal method [3] using ideal and magnetic-core instrument transformers.

It is important to note that the mentioned drawback emanates from the possibility of inclusion of one or more erroneous equations in the minimal number of fault equations that those method use. This means the removal of such equations would make fault location unsolvable. Therefore, inaccurate results for close-in faults are essentially expected by any conventional fault location method, unless it is capable of detecting and correcting erroneous measurements [2]. This could be achieved at the expense of spending much more computational effort, if the instrument transformer models and exact parameters are available [2].

To be more specific, the very well-known conventional method proposed in [3] is used as an example. A 1-ph-g fault at 95% of line 21-22 of 39-bus system is studied. The faulted-phase voltage angle at the fault location is considered to be 45° upon the fault inception. The voltage and current signals obtained via ideal and magnetic-core instrument transformers at terminal 22, and the estimation error are shown in Figs. 4 to 6, respectively. It can be seen that the estimation error of the proposed algorithm in [3] is considerable for this fault. In fact, instrument transformers transients have increased the error of fault location by affecting the estimated phasors.

TABLE II
FAULT LOCATION RESULTS ON 39-BUS SYSTEM

Fault Area	Northern Fault Area	Western Fault Area	Eastern Fault Area
Fault Type	Estimation Error % (μ,σ,max)		
1-ph-g	(0.09,0.02,0.26)	(0.10,0.02,0.25)	(0.11,0.02,0.29)
2-ph	(0.08,0.02,0.23)	(0.08,0.02,0.22)	(0.09,0.02,0.23)
2-ph-g	(0.07,0.01,0.21)	(0.08,0.02,0.22)	(0.08,0.02,0.24)
3-ph-g	(0.05,0.01,0.18)	(0.06,0.01,0.19)	(0.06,0.01,0.18)
All in Total	(0.07,0.02,0.26)	(0.08,0.02,0.25)	(0.08,0.02,0.29)

It should be also noted that not all the wide-area fault location methods have a satisfactory performance as the proposed method has in dealing with imperfect measurements. For example, the method proposed in [17] mainly takes advantage of the closest measurements to the fault due to its formulation nature. Accordingly, its performance is similar to those of conventional methods in case of close-in faults. Some others use an offline created simulation database to find the most fitting waveforms to the recorded fault signals [22-24]. Creation and continuous update of such database are not practical in the case of relatively large-scale power systems. More than two synchrophasor measurements cannot be readily used for fault location by the approach proposed in [25] and [26]. Overall, a major disadvantage of the above-mentioned wide-area fault location methods is that inclusion of bad data cannot be readily handled by them.

Not only do the more recent algorithms such as [18]-[20] enforce more computational burden, but also they are easily outperformed by the proposed method. The reason for this is because references [18]-[20] approximately model electric machines while the method proposed in this paper involves no approximation. It can be seen that the proposed method pinpoints the fault with accuracy better than 0.07% regardless of the fault distance along line 21-22. This is due to the fact that erroneous measurements of close instrument transformers, if any, are easily identified and removed from the measurement set. Accordingly, the fault location result becomes more accurate by taking advantage of data mainly provided by the farther measurement devices.

B. General Evaluation of the Proposed Method

The 39-bus system is equipped with 11 PMUs that make it fully observable [39], [40]. As shown in Fig. 3, this system has been divided into three regions with respect to its geographical characteristics, which are named northern, western and eastern areas. To scrutinize the proposed fault location method, an extensive number of fault cases are simulated in each area. These fault areas include 7, 18 and 9 transmission lines, respectively. Each of the system areas is modeled as a stand-alone sub-system using the technique proposed earlier. To make the evaluation comprehensive, various fault types with different fault resistances from 0 to 50 Ω are simulated at five points on each line. Moreover, six fault inception angles in the range $(-\pi,\pi]$ are examined for every case.

A total of more than 3000 fault cases are simulated in this part. In all the simulated cases, the faulted line is successfully identified by the proposed method. Table II summarizes the average, standard deviation and maximum of estimation errors for various fault types. As can be seen, the average estimation error is below 0.11% for all the conducted simulations. It should be also pointed out that the fault type is always identified correctly. These accurate results are achieved after detection and removal of erroneous measurements using the Normalized Residual test [35].

TABLE III
FAULT LOCATION RESULTS ON 118-BUS SYSTEM

Terminals Located in Fault Area	PMU Locations	Estimation Error (%) (μ,σ,max)
1,2,3,4,5,6,7,8,9,10,11,12,13, 14 ,15,16,17,18,19, 20,21,22, 23, 25,26,27,28,29, 30,31,32, 34,113, 114,115,117	1,5,9,12,15,17,21 23,28,30,115	(0.11, 0.03, 0.28)
15,33,34,35,36,37,38,39,40,41, 42,43, 44,45,46,47,48,49,50, 51,52,53,54,55,56,57,58,59, 60,61,62,63,64,65,66,67	15,34,35,38, 40,43,47,49,53, 56,63,62,67	(0.14, 0.02, 0.31)
23,24,38,47,49,68,69,70,71,72, 73,74,75,76,77,78,79,80,81,82, 83,84,85,86,87,88,89,90, 91, 92,93,94,95,96,97,98,99,100, 101, 102, 03,104,105,106,107, 108,109,110,111,112, 116,118	23,38,47,49, 71,75,78,80, 85,86,90,94, 102,105,110	(0.12, 0.02, 0.27)

The tabulated results in Table II are related to the fault cases including a fixed resistance. A number of simulations with a variable fault resistance including transient components [2] have been also conducted. The results show that although the nonlinearity of fault resistance deteriorates the accuracy, the estimation error hardly exceeds 1%.

Wide-area fault location methods usually use a simplified model for electric machines, i.e., a constant source in connection with a fixed impedance, to construct the bus impedance matrix. Such approximation requires some of the machine parameters, and loses its accuracy as the time moves on. The reason is that the time-varying nature of machine impedance, rotor saliency, automatic voltage regulation action and some other factors are neglected in the simplified model. For example, if terminals 10 and 11 have no PMUs, the approximate model of generators 31 and 32 should be used for applying wide-area fault location in the 39-bus system. Simulation results show that this could increase the estimation error up to 1% in a few cases. As proposed in this paper, however, having PMUs at machine terminals enables replacing them with exact sources and thereby increasing the fault location accuracy.

In order to evaluate the proposed method performance when applied to large-scale power systems, the 118-bus system is also examined here. Based on the geographical criteria along with engineering judgment, this system is divided into three fault areas as shown in Table III. More than 2000 fault cases are simulated in each area and the proposed method is applied to pinpoint the fault. As tabulated, the average estimation error is less than 0.14% for all of the conducted simulations. Further analysis shows that if the fault location is carried out without dividing the system into three fault areas using the proposed method, the average estimation error would be around 0.42%. The reason is because the simplified model commonly used for electric machines modeling in fault location studies is not

TABLE IV
EVALUATION OF SOLVABILITY CONDITIONS FOR LINES WITH RANK-DEFICIENT COEFFICIENT MATRIX

Faulted Line	$\text{rank}(\mathbf{H})$	$\text{rank}(\mathbf{H}^{\text{I}})$	$\text{rank}\begin{pmatrix}\begin{bmatrix}\mathbf{H}^{\text{I}}\\ \boldsymbol{\Upsilon}^{\text{Nb}}_{\text{i,j}}\end{bmatrix}\\ \boldsymbol{\Upsilon}^{\text{Nb}}_{\text{j,i}}\end{pmatrix}$	Condition I	Condition II
2-3	5	4	5	×	×
3-4	5	5	5	×	✓
3-18	5	4	5	×	×
4-5	5	4	5	×	×
4-14	5	4	5	×	×
5-6	6	5	5	✓	✓
5-8	6	5	5	×	✓
6-11	5	4	5	×	×
10-11	5	5	5	×	✓
10-13	5	5	5	×	✓
13-14	5	5	5	×	×

quite accurate. As proposed in this paper, it is desirable to replace electric machines with their equivalent sources in case their associated terminals are equipped with PMUs. This would reduce the average estimation error again to around 0.14%, although the whole 118-bus system is considered as the fault-area.

C. Solvability of Fault Equations

To carry out wide-area fault location, it is not necessary that all fault equations be uniquely solvable. Injected currents from the boundary terminals to the fault area are amongst the unknowns of (14) to be calculated. The fault distance can be successfully located if this system of equations is uniquely solvable for $\Delta \mathrm{J}_{\mathrm{i,j}}$ and $\Delta \mathrm{J}_{\mathrm{j,i}}$, and also the superimposed voltages can be calculated from (17) and (18). As explained earlier, it is not necessary that all the boundary terminals be equipped with PMUs as long as there exist enough independent equations in the system of equations (14).

In this part, a number of short-circuit faults are simulated at ten points on line 7-8 of 39-bus system. Fault location is carried out without considering synchrophasors measured at boundary terminals 2, 14 and 17. The obtained results confirm successful fault location in all the cases even though the entire boundary terminals are not equipped with PMUs. In this respect, the average estimation error with and without PMUs at terminals 2, 14 and 17 are 0.09 and 0.13, respectively.

The western fault area of 39-bus system has five boundary terminals, namely terminals 2, 6, 10, 14 and 17. As an example, the introduced solvability conditions are evaluated in Table IV for cases in which only terminals 2 and 6 are equipped with PMUs. For lines 1-2, 1-39, 6-7, 7-8, 8-9 and 9-39, the rank of coefficient matrix **H** is full, that is 7 here, and both solvability conditions hold. These cases have not been included in the table because it is safe to say that fault location is feasible for those lines without checking individually the solvability conditions. It can be seen from the table that the fault location solvability conditions hold for line 5-6, although the rank of the respective coefficient matrix **H** is 6. This means that fault distance can be successfully pinpointed for any fault on this line even though the system of equations associated to it has infinitely many solutions.

V. CONCLUSIONS

A method is proposed in this paper to determine the fault identity, i.e., the fault type, faulted line and fault location on it, using available synchrophasors. To reduce the computational complexity, and to simplify the exchange and processing of data between utilities, the whole process is confined to the fault area. A low-demanding technique is proposed to suitably replace the remote portions of the system and construct an equivalent fault sub-system. The fault equations become linear by defining appropriate auxiliary variables. Taking advantage of partial solvability of system of linear equations, two necessary and sufficient conditions are introduced for assessing the fault location feasibility in the offline stage. It is shown that for being able to locate the fault using a given set of PMUs, it is not required that the whole system of equations be uniquely solvable. Overall, the major achievements of the proposed method can be outlined as follows:

- Linearity of the proposed formulation removes concerns about non-convergence and demanding solving process involved in nonlinear problems.
- Restricting calculations to the fault sub-system removes a huge portion of modeling complexity and associated uncertainties.
- Topology data and parameters of the portions being replaced are not needed.
- The proposed method determines the fault identity, and does not require all of the system terminals to be equipped with PMUs.
- Necessary and sufficient conditions are introduced to assess the feasibility of fault location by any set of PMUs.
- Both voltage and current measurements are taken into account since gross errors can be easily identified and removed in the proposed linear framework.
- The proposed wide-area method provides accurate results even in presence of instrument transformers transients.

Acknowledgment

The first author would like to thank Dr. Ahmad Salehi Dobakhshari of University of Guilan, Dr. Peyman Jafarian, Mr. Sayyed Mohammad Hashemi and Mr. Mohsen Kalantar Neyestanaki of Iran Grid Management Co. (IGMC) for their insightful comments on the paper.

REFERENCES

[1] S. H. Horowitz, and A. G. Phadke, Power System Relaying. John Wiley and Sons, 3rd ed., 2008.
[2] M. M. Saha, J. J. Izykowski, and E. Rosolowski, Fault Location on Power Networks, 1st ed., Springer: London, 2010.
[3] A. T. Johns, S. Jamali, "Accurate fault location technique for power transmission lines," in Proc. IEE Gen., Transm. Distrib., vol. 137, no. 6, pp. 395–402, Nov. 1990.
[4] V. Terzija, Z. M. Radojevic, and G. Preston, "Flexible synchronized measurement technology-based fault locator," IEEE Trans. on Smart Grid, vol. 6, no. 2, pp. 866-873, Mar. 2015.
[5] C. J. Lee, J. B. Park, J. R. Shin. Z. M. Radojevie, "A new two-terminal numerical algorithm for fault location, distance protection, and arcing fault recognition." IEEE Trans. Power Syst., vol. 21, no. 3, pp. 1460–1462, Aug. 2006.

[6] E. G. Silveira, C. Pereira, "Transmission line fault location using two terminal data without time synchronization." IEEE Trans. Power Syst., vol. 22, no. 1, pp. 498–499, Feb. 2007.
[7] B. Mahamdedi, M. Sanaye-Pasand, S. Azizi, and J. G. Zhu, "Unsynchronised fault-location technique for three-terminal lines," IET Gen., Transm. Distrib., vol. 9, no. 15, pp. 2099-2107, Jun. 2015.
[8] J. Izykowski, E. Rosolowski, M. M. Saha, M. Fulczyk, and P. Balcerek, "A fault-location method for application with current differential relays of three-terminal lines," IEEE Trans. Power Del., vol. 22, no. 4, pp. 2099–2106, Oct. 2007.
[9] A. J. Mazon, I. Zamora, J. Gracia, K. J. Sagastebeitia, and J. R. Saenz, "Selecting ANN structures to find transmission faults.," IEEE Comput. Appl. Power, vol. 14, no. 3, pp. 44–48, Jul. 2001.
[10] I. Zamora, J. F. Minambres, A. J. Mazon, R. Alvarez-Isasi and J. Lazaro, "Fault location on two-terminal transmission lines based on voltages", in Proc. IEE Gen., Transm. Distrib., vol. 143, no. 1, pp. 1–6, Jan. 1996.
[11] Chen, J. C. Maun, "Artificial neural network approach to single-ended fault locator for transmission lines." IEEE Trans. Power Syst., vol. 15, no. 1, pp. 370–375, Feb. 2000.
[12] R. Salat, S. Osowski, "Accurate fault location in the power transmission line using support vector machine approach." IEEE Trans. Power Syst., vol. 19, no. 2, pp. 979–986, May 2004.
[13] M. Farshad and J. Sadeh, "Accurate single-phase fault-location method for transmission lines based on k-nearest neighbor algorithm using one-end voltage," IEEE Trans. Power Del., vol. 27, no. 4, pp. 2360–2367, Oct. 2012.
[14] R. Razzaghi, G. Lugrin, H. Manesh, C. Romero, M. Paolone and F. Rachidi, "An efficient method based on the electromagnetic time reversal to locate faults in power networks." IEEE Trans. Power Del. vol. 28, no. 3, pp. 1663-1672, Nov. 2013.
[15] S. Azizi, M. Sanaye-Pasand, M. Abedini, and A. Hassani, "A traveling-wave-based methodology for wide-area fault location in multiterminal DC systems," IEEE Trans. Power Del. vol. 29, no. 6, pp. 2552–2560, Aug. 2014.
[16] S. Azizi, S. Afsharnia, and M. Sanaye-Pasand, "Fault location on multi-terminal DC systems using synchronized current measurements," International Journal of Electrical Power & Energy Systems, vol. 63, pp. 779-786, Dec. 2014.
[17] K. P. Lien, C. W. Liu, C. S. Yu, and J. A. Jiang, "Transmission network fault location observability with minimal PMU placement," IEEE Trans. Power Del., vol. 21, no. 3, pp. 1128-1136, Jul. 2006.
[18] A. S. Dobakhshari and A. M. Ranjbar, "A wide-area scheme for power system fault location incorporating bad data detection," IEEE Trans. Power Del., vol. 30, no. 2, pp. 800–808, Apr. 2015.
[19] A. S. Dobakhshari, and A. M. Ranjbar, "A novel method for fault location of transmission lines by wide-area voltage measurements considering measurement errors," IEEE Trans. on Smart Grid, vol. 6, no. 2, pp. 874-884, Mar. 2015.
[20] S. Azizi, M. Sanaye-Pasand, "A straightforward method for wide-area fault location on transmission networks," IEEE Trans. Power Del. vol. 30, no. 1, pp. 441–445, Feb. 2015.
[21] A. S. Dobakhshari and A. M. Ranjbar, "Application of synchronized phasor measurements to wide-area fault diagnosis and location", IET Gen., Transm. Distrib., vol. 8, no. 4, pp. 716-729, Apr. 2014.
[22] M. Kezunovic and Y. Liao, "Fault location estimation based on matching the simulated and recorded waveforms using genetic algorithms," in Proc. Int. Conf. Develop. Power Syst. Protect., RAI, Amsterdam, the Netherlands, Apr. 2001.
[23] Z. Galijasevic and A. Abur, "Fault location using voltage measurements," IEEE Trans. Power Del., vol. 17, no. 2, Apr. 2002.
[24] A. S. Dobakhshari, and A. M. Ranjbar, "A circuit approach to fault diagnosis in power systems by wide-area measurement system," Int. Trans. Elect. Energy Syst., vol. 23, no. 8, pp. 1272–1288, Nov. 2013.
[25] Y. Liao, "Fault location for single-circuit line based on bus-impedance matrix utilizing voltage measurements," IEEE Trans. Power Del., vol. 23, no. 2, pp. 609–617, Apr. 2008.
[26] N. Kang and Y. Liao, "Double-circuit transmission-line fault location with the availability of limited voltage measurements," IEEE Trans. Power Del., vol. 27, no. 1, pp. 325–336, Jan. 2012.
[27] S. Azizi, M. Sanaye-Pasand, and M. Paolone, "Locating faults on untransposed, meshed transmission networks using a limited number of synchrophasor measurements," IEEE Trans. Power Syst., vol. PP, no. 99, pp. 1–11, 2016.
[28] G. Feng and A. Abur, "Identification of faults using sparse optimization," in Proc. 52nd Annual Allerton Conference on Communication, Control, and Computing, 30 Sep.-3 Oct. 2014.
[29] Q. Jiang, X. Li, B. Wang, and H. Wang, "PMU-based fault location using voltage measurements in large transmission networks," IEEE Trans. Power Del., vol. 27, no. 3, pp. 1644–1652, Jul. 2012.
[30] M. Majidi, M. Etezadi-Amoli, M. S. Fadali, "A sparse-data-driven approach for fault location in transmission networks," IEEE Trans. Smart Grid, vol. PP, no. 99, pp. 1–9, 2015.
[31] A. Esmaeilian and M. Kezunovic, "Fault location using sparse synchrophasor measurement of electromechanical wave oscillations," IEEE Trans. Power Del., vol. PP, no. 99, pp. 1–1, 2016.
[32] N. D. Tleis, Power Systems Modeling and Fault Analysis: Theory and Practice. 7th ed., Oxford, UK: Newnes, 2008.
[33] M. K. Neyestanaki and A. M. Ranjbar, "An adaptive PMU-based wide area backup protection scheme for power transmission lines," IEEE Trans. Smart Grid, vol. 6, no. 3, pp. 1550–1559, May 2015.
[34] C. A. Desoer and E. S. Kuh, Basic Circuit Theory, New Delhi: Tata McGraw-Hill, 2009.
[35] A. Abur, and A. G. Exposito, Power System State Estimation: Theory and Implementation, Marcel Dekker, Inc. 2004.
[36] C. D. Meyer, Matrix Analysis and Applied Linear Algebra, SIAM, 2001.
[37] R. D. Zimmerman, C. E. Murillo-Sanchez, and D. Gan, "MATPOWER, a MATLAB Power System Simulation Package". ver. 3.2, 2007. [Online]. Available: http://www.pserc.cornell.edu/matpower/.
[38] DIgSILENT Power Factory, Version 14.1, DIgSILENT GmbH, 2008.
[39] S. Azizi, A. S. Dobakhshari, S. A. N. Sarmadi, and A. M. Ranjbar. "Optimal PMU placement by an equivalent linear formulation for exhaustive search," IEEE Trans. on Smart Grid, vol. 3, no. 1, pp. 174-182, Mar. 2012.
[40] S. Azizi, A. S. Dobakhshari, S. A. N. Sarmadi, A. M. Ranjbar, and G. B. Gharehpetian, "Optimal multi-stage PMU placement in electric power systems using Boolean algebra," Int. Trans. Elect. Energy Syst., vol. 24, no. 4, pp. 562–577, Apr. 2014.

Sadegh Azizi (S'12) received the B.Sc., M.Sc. and Ph.D. degrees all in electrical engineering from K. N. Toosi University of Technology, Sharif University of Technology, and the University of Tehran, Tehran, Iran in 2007, 2010 and 2016, respectively.

Dr. Azizi was with the Energy and System Study Center, Monenco Iran Consulting Engineers Co., from 2009 to 2011 and the Iran Grid Management Co. (IGMC), Tehran, Iran, from 2013 to 2016. He has also been collaborating with the Distributed Electrical Systems Laboratory (DESL) at the Swiss Federal Institute of Technology of Lausanne (EPFL) since October 2014. Currently, he is a postdoctoral research associate at the University of Manchester, Manchester, U.K. His research interests include applications of wide-area monitoring, protection and control systems, digital protective relays, and applications of power electronics in power systems.

Majid Sanaye-Pasand (M'98–SM'05) received the electrical engineering degree from the University of Tehran, Tehran, Iran, in 1988, and the M.Sc. and Ph.D. degrees in electrical engineering from the University of Calgary, Calgary, AB, Canada, in 1994 and 1998, respectively.

Currently, he is a Professor at the School of Electrical and Computer Engineering, University of Tehran, where he is also with the Control and Intelligent Processing Center of Excellence. His research interests include power system analysis and control, digital protective relays, and application of artificial intelligence.